5-30-2003

RNase L Mediates Transient Control of The Interferon Response Through Modulation of The Double-stranded RNA-Dependent Protein Kinase PKR

Khalid S.A. Khabar
King Faisal Specialist Hospital and Research Center

Yunus M. Siddiqui
King Faisal Specialist Hospital and Research Center

Fahad Al-Zoghaibi
King Faisal Specialist Hospital and Research Center

Latifa al-Haj
King Faisal Specialist Hospital and Research Center

Mohammed Dhalla
King Faisal Specialist Hospital and Research Center

Publisher's Statement

This research was originally published in Journal of Biological Chemistry. Khalid S. A. Khabar, Yunus M. Siddiqui, Fahad Al-Zoghaibi, Latifa Al-Haj, Mohammed Dhalla, Aimin Zhou, Beihua Dong, Mark Whitmore, Jayashree Paranjape, Mohammed N. Al-Ahdal, Futwan Al-Mohanna, Bryan R. G. Williams and Robert H. Silverman. RNase L Mediates Transient Control of The Interferon Response Through Modulation of The Double-stranded RNA-Dependent Protein Kinase PKR. Journal of Biological Chemistry. 2003; 278, 20124-20132. © the American Society for Biochemistry and Molecular Biology."

See next page for additional authors

THE JOURNAL OF BIOLOGICAL CHEMISTRY
Vol. 278, No. 22, Issue of May 30, pp. 20124–20132, 2003
Printed in U.S.A.

RNase L Mediates Transient Control of the Interferon Response through Modulation of the Double-stranded RNA-dependent Protein Kinase PKR*

Received for publication, August 27, 2002, and in revised form, January 16, 2003
Published, JBC Papers in Press, February 11, 2003, DOI 10.1074/jbc.M208766200

Khalid S. A. Khabar‡§¶, Yunus M. Siddiqui‡, Fahad al-Zoghaibi‡, Latifa al-Haj‡, Mohammed Dhalla‡, Aimin Zhou‖, Beihua Dong§, Mark Whitmore§, Jayashree Paranjape§, Mohammed N. Al-Ahdal‡, Futwan Al-Mohanna‡, Bryan R. G. Williams§, and Robert H. Silverman§

From the ‡Department of Biological and Medical Research, King Faisal Specialist Hospital and Research Center, Riyadh 11211, Saudi Arabia, the §Department of Cancer Biology, Lerner Research Institute, Cleveland Clinic Foundation, Cleveland, Ohio 44195, and the ‖Department of Chemistry, Cleveland State University, Cleveland, Ohio 44115

The transient control of diverse biological responses that occurs in response to varied forms of stress is often a highly regulated process. During the interferon (IFN) response, translational repression due to phosphorylation of eukaryotic initiation factor 2*α*, eIF2*α*, by the double-stranded RNA-dependent protein kinase, PKR, constitutes a means of inhibiting viral replication. Here we show that the transient nature of the IFN response against acute viral infections is regulated, at least in part, by RNase L. During the IFN antiviral response in *RNase L*-null cells, PKR mRNA stability was enhanced, PKR induction was increased, and the phosphorylated form of eIF2*α* appeared with extended kinetics compared with similarly treated wild type cells. An enhanced IFN response in *RNase L*-null cells was also demonstrated by monitoring inhibition of viral protein synthesis. Furthermore, ectopic expression of RNase L from a plasmid vector prevented the IFN induction of PKR. These results suggest a role for RNase L in the transient control of the IFN response and possibly of other cytokine and stress responses.

Negative feedback mechanisms are essential for maintaining transient responses such as those of the immune response by attenuating undesirable outcomes resulting from prolonged responses. Different negative regulatory pathways of interferon (IFN)[1] and cytokine responses exist in mammalian cells such as those of the suppressors of signals (1) and mRNA turnover regulation by the AU-rich elements in the 3′-untranslated regions (2). The IFN antiviral response is a highly regulated process involving the transient inhibition of viral and cellular protein synthesis. The translational inhibition is mediated predominately by the activity of PKR, the double-stranded RNA-dependent protein kinase. PKR is a serine/threonine protein kinase of 65 and 68 kDa in murine and human cells, respectively, that is induced by IFN treatment of cells and phosphorylates itself and other proteins, notably eIF2*α*, in response to viral double-stranded RNA (3). DsRNA is produced as the replicative intermediates of many RNA viruses and also by annealing of complementary RNA strands transcribed from some DNA viruses (3). Phosphorylated eIF2*α* sequesters the guanine nucleotide exchange factor, eIF2B, which becomes trapped as inactive complex with GDP resulting in translational arrest (4, 5).

Among the principal effectors of the IFN-induced antiviral state are the 2′,5′-oligoadenylate (2-5A) synthetases that convert ATP to 2-5A, activators of RNase L, in response to viral double-stranded RNA (6, 7). Thus, 2-5A is an alarmone that alerts the cells to the presence of virus by signaling to RNase L. Both RNase L and PKR have been implicated in the action of IFN-*α* against a variety of viruses (reviewed in Refs. 8 and 9). RNase L is widely distributed in different tissues, and it has been suggested that low levels of 2-5A lead to RNase L-mediated selective degradation of viral mRNA (10), whereas higher levels may lead to broader effects such as cleavage of 18 S and 28 S ribosomal RNAs (11). During the course of experiments on the role of RNase L in the inhibition of viral protein synthesis during acute infections, we observed that an absence of RNase L led to selective stabilization of PKR mRNA, extended kinetics of eIF2*α* phosphorylation, and potent inhibition of viral protein synthesis. Our findings suggest that RNase L truncates and limits the induction of PKR, possibly contributing to the transient nature of the IFN response against viral infections.

EXPERIMENTAL PROCEDURES

Cell Culture, Viral Infections, and IFN Treatments—RNase L$^{+/+}$ and *RNase L*$^{-/-}$ mouse embryonic fibroblast (MEF) cell lines were of mixed or C57BL/6 genetic backgrounds. The cell lines are post-crisis derivatives of primary MEFs as described previously (12). MEFs were cultured in DMEM with high glucose supplemented with 10% FBS and antibiotics (Invitrogen, Gaithersburg, MD). Bone marrow macrophages collected from the femurs of *RNase L*$^{+/+}$ and *RNase L*$^{-/-}$ mice, both on a background of C57BL/6, were cultured in L-cell-conditioned medium for 8 days and plated at a density of 10^6 cells per 10-cm plate. WISH cell line (HeLa markers) was obtained from the American Type Culture Collection (ATCC, Rockville, MD) and cultured in RPMI 1640 supplemented with 10% FBS and antibiotics.

* This work was supported in part by awards from the National Institutes of Health (NCI Grant CA44059 to R. H. S. and NIAID Grant AI343039 to B. R. G. W.) and the King Faisal Specialist Hospital and Research Center (to K. S. A. K.). The costs of publication of this article were defrayed in part by the payment of page charges. This article must therefore be hereby marked "*advertisement*" in accordance with 18 U.S.C. Section 1734 solely to indicate this fact.

¶ To whom correspondence should be addressed: Interferon and Cytokine Research Unit, King Faisal Specialist Hospital and Research Center, P. O. Box 3354, MBC-03, Riyadh 11211, Saudi Arabia. Tel.: 966-1-442-7876; Fax: 966-1-442-7858 (or -54); E-mail: khabar@kfshrc.edu.sa.

[1] The abbreviations used are: IFN, interferon; PKR, double-stranded RNA-dependent protein kinase; 2-5A, 2′,5′-oligoadenylate; MEF, mouse embryonic fibroblast; DMEM, Dulbecco's modified Eagle's medium; FBS, fetal bovine serum; EMCV, encephalomyocarditis virus; VSV, vesicular stomatitis virus; BSA, bovine serum albumin; STAT, signal transducers and activators of transcription; HRP, horseradish peroxidase; ANOVA, analysis of variance; CMS, Cytosensor microphysiometer system; HSV-1, herpes simplex virus, type 1; eIF-2*α*, *α* subunit of eukaryotic initiation factor-2; dsRNA, double-strand RNA; OAS, 2′,5′-oligoadenylate synthetase; m.o.i., multiplicity of infection.

Encephalomyocarditis virus (EMCV) and vesicular stomatitis virus (VSV, Indiana strain) were obtained from the ATCC (Manassas, VA). Virus preparations were clarified by low speed centrifugation, filtered through 0.22-μm membranes for sterility, and titrated on VERO (African Green Monkey Kidney cell line, ATCC) with resultant titers of 2×10^9 and 8×10^8 plaque forming units/ml for EMCV and VSV, respectively. Viruses were aliquoted and stored at −70 °C until use.

Hybrid IFN-α BBDB, equally active on mouse and human cells, was a generous gift from H. K. Hochkeppel (Norvatis Pharma AG) (13). The specific activity, determined by titrating on human amnion cells (WISH) calibrated with National Institutes of Health standard IFN, Gxa01-901-535, was 1.3×10^9 IU/mg using the manufacturer's reported amount of pure IFN weight.

Monitoring Phosphorylation of the α Subunit of eIF2—Cells were incubated with or without IFN-α (1000 units/ml). Proteins were extracted in ice-cold lysis buffer. Kinase reactions were in 20 mM Tris-HCl, pH 7.5, 0.3 mg/ml BSA, 5% glycerol, 100 IU aprotinin, 10 μM EDTA, 50 mM KCl, 2 mM MgCl, 2 mM $MnCl_2$, 100 μM ATP, and 100 ng/ml of poly(I)·poly(C) and incubated at 30 °C for 30 min. To monitor eIF2α levels, cells were incubated with or without IFN-α and infected with EMCV (m.o.i. = 10) for 0.5, 1, 2, or 4 h followed by lysing the cells in ice-cold lysis buffer. Proteins were separated on SDS-10% acrylamide gels and transferred to polyvinylidene difluoride membranes (Bio-Rad, Richmond, CA). Membranes were blocked with buffer containing 2% BSA/0.5% Tween-20 and probed with anti-phospho-eIF2-α antiserum (Cell Signaling Technology, Beverly, MA) by incubating the membrane overnight at 4 °C with antibody diluted in the blocking buffer. The antibody specifically detects eIF2α only when phosphorylated at serine 51, because the antibody was raised against a peptide corresponding to residues surrounding Ser-51 of human eIF2α. Secondary antibody (anti-rabbit IgG labeled with horseradish peroxidase) was used for immunodetection and visualization (ECL, Amersham Biosciences, Buckingham, UK). Rabbit Antibodies to total eIFα (Santa Cruz Biotechnology) were also used to probe Western blots.

Monitoring Viral Protein Synthesis—IFN-mediated inhibition of viral protein synthesis was determined in the presence of actinomycin D to selectively inhibit cellular transcription and thereby reduce cellular protein synthesis. Confluent MEFs (2×10^5 cells per well) in 24-well plates (Linbro, Flow Laboratories) were incubated in maintenance medium (DMEM plus 2% FBS) in the absence or presence of IFN-α at 1000 units/ml for 20 h. EMCV was incubated with the cells for 1 h. Unadsorbed virus was removed, and cells were incubated for 4 h with maintenance medium containing 5 μg/ml of actinomycin D (Sigma, St. Louis, MO). The medium was replaced with cysteine/methionine-free medium supplemented with 6 μCi of [^{35}S]cysteine/methionine (Promix, Amersham Biosciences). The cells were incubated for a further 1.5 h, media were removed, and proteins were extracted in gel sample buffer.

Infectious Virus Yield Assays—Confluent cells were infected for 1 h, unadsorbed virus was removed by washing monolayers with PBS containing 2% FBS, and infections were continued in DMEM with high glucose supplemented with 5% FBS and antibiotics. Cell lysates were obtained by repeated freezing and thawing, and supernatants (containing both intracellular and extracellular viral particles) were collected after centrifugation at $300 \times g$ at 4 °C. Infectious virus in the clarified supernatants were quantitated by plaque assays after titration on confluent monolayers of VERO cells grown in 24-well plates with overlay MEM medium containing agar (Sigma). The plates were fixed and stained with crystal violet, and plaques were counted.

Immunoprecipitations and Autophosphorylation of PKR—Confluent cells (4×10^5 cells per well) in 12-well tissue culture dishes (Linbro) were incubated with or without IFN-α (1000 units/ml) for different periods of time. Cultures were incubated for 24 h in methionine-free minimal essential medium (Invitrogen) supplemented with 2% dialyzed FBS and 10 μCi of [^{35}S]methionine (Amersham Biosciences). After washing, cells were lysed in buffer containing 1% Triton X-100. Lysates were incubated with anti-PKR antibody (Santa Cruz; 1/250 dilution), and immune complexes containing PKR were immobilized on protein-A-Sepharose beads (Amersham Biosciences) for 1 h at 4 °C. PKR was eluted by boiling in gel sample buffer and incubated with [γ-^{32}P]ATP and poly(dI)·poly(dC) in a kinase reaction buffer for 30 min.

SDS-PAGE—Equal amounts, as determined by the Bradford method (Bio-Rad, Richmond, CA), of proteins or equal amounts of the immunoprecipitation lysates were electrophoresed in 12% SDS-PAGE gels. The gels were fixed overnight, washed, dried, and visualized by autoradiography (Kodak XAR film, Kodak, Rochester, NY) at −70 °C. Protein molecular weight markers (^{14}C-methylated, 14–220 kDa) were used to verify the size of viral proteins. In the case of phosphorylated STAT-1, protein was visualized using the ECL chemiluminescence kit (Amersham Biosciences).

Assay of PKR Levels in Mice Treated with IFN-α—Female *RNase* $L^{+/+}$ (Jackson Lab, C57/bl6) and female *RNase* $L^{-/-}$ (C57/bl6) mice at 10 weeks of age were injected by the intraperitoneal route with 5×10^5 units of IFN-α (BBDB) in 200 μl of PBS. Organs (spleen and thymus) were removed from sacrificed mice that were either untreated or IFN-α treated for 16, 48, and 72 h. Protein (200 μg) prepared from frozen (−70 °C) spleens and thymuses were separated by SDS-PAGE, transferred to membrane, and probed with rabbit anti-human PKR (cross-reactive with mouse PKR) and goat anti-rabbit IgG-horseradish peroxidase (HRP, Invitrogen, Carlsbad, CA) and visualized (ECL, Amersham Biosciences). The same blots were re-probed with goat anti-β-actin anti-goat-HRP.

Transient Transfection of Human RNase L—Semi-confluent WISH (HeLa markers) line was assessed for transfection efficiency using green fluorescent protein vector (Invitrogen). Semi-confluent WISH (HeLa markers) was transfected with either pcDNA3.1 vector or pcDNA3.1 containing full-length human RNase L cDNA. Transfections were performed in serum-free medium using LipofectAMINE 2000 (Life Technologies, Inc.) for 6 h followed by replacing the medium with serum-supplemented medium. After 18 h incubation, human recombinant IFN-α2a (500 IU/ml) was added for additional 18 h. PKR levels were visualized by confocal microscopy using specific antibody to PKR (Santa Cruz Biotechnology Co., Santa Cruz, CA) or by Western blotting.

Cytosensor Microphysiometer System—Cells were incubated onto capsule cups for use with a Cytosensor (Molecular Devices, Sunnyvale, CA) overnight at 37 °C in CO_2 incubator. The cells were then transferred into the silicon-containing sensor chambers of the Cytosensor and pumped with running buffer comprising low buffered (1 mM phosphate) RPMI medium supplemented with 1% BSA at a flow rate of 100 μl/min and pump cycle was 2 min. The pump cycle consisted of on and off cycles: in the off cycle the fluid flow was periodically halted allowing a build-up of protons (due to acid metabolites as a result of receptor activation) in the chamber; in the on cycle the pump allowed fluid to be resumed and the acid was flushed out of the chamber. This cycle was repeated, and the basal rate of acidification was first measured in the absence of IFN-α. The acidification rate is the output of protons from the cells. The acidification rates due to IFN-α were measured; using a 2-min pump protocol and five repeat cycles, before and after IFN-α treatment to determine the relative changes in acidification rates due to IFN-α. The operation of the apparatus was carried out as recommended by the manufacturer. Data were processed by software supplied by the same manufacturer, and data were exported as an Excel spreadsheet file to GraphPad Prism software (San Diego, CA) for graphics.

Measurement of STAT-1 Tyrosine Phosphorylation—Cells (10^7) were extracted in a cold lysis buffer, and the lysates were incubated with antibody to STAT-1 (Santa Cruz Biotechnology) or normal serum. Immunoprecipitates were collected, and proteins were separated by SDS-PAGE and transferred to nitrocellulose. Blots were washed and blocked with 4% BSA in PBS for 1 h at room temperature. Antibody to phosphotyrosine (1 μg/ml, Zymed Laboratories) was incubated with the membranes at 4 °C for 18 h followed by incubation for 2 h with secondary horseradish peroxidase-conjugated antibody.

Immunofluorescence and Confocal Microscopy—Cells were formaldehyde-fixed and incubated with primary antibody to PKR (Santa Cruz Biotechnology, 1/50 dilution) for 16 h at 4 °C. The cells were then washed three times to remove unbound antibodies. Fluorescein isothiocyanate secondary antibody (1/100 dilution, 1 h at 37 °C) was subsequently used. Cells were then washed three times in PBS, and the immunofluorescence associated with the cells was imaged using a confocal laser scanning microscopy (Leica-Kaki, Saudi Arabia).

RNA Preparation and Northern Blot Analysis—Total RNA was extracted using TRIzol reagent (Molecular Research Center, Cincinnati, OH), and 15 μg was electrophoresed through a 1.2% agarose/2.2 M formaldehyde gel. Transfer of RNA was performed overnight using Zeta Probe nylon membranes (Bio-Rad, Hercules, CA). Membranes were baked for 2 h in a vacuum oven at 80 °C and prehybridized in Express Hyb solution (Clontech, Palo Alto, CA) in a Hybaid hybridization oven at 68 °C (Labnet, Woodbridge, NJ). cDNA probes specific for PKR mRNA were labeled with [α-^{32}P]dCTP (Amersham Biosciences) using a nick translation kit (Invitrogen). A 40-mer hybridization oligonucleotide probe (Clontech) specific for β-actin mRNA was labeled with [γ-^{32}P]ATP using T4 polynucleotide kinase (Promega). The blots were exposed to x-ray film, and the autoradiograms were subsequently developed. RNA signals were measured with a densitometer (Bio-Rad, Hercules, CA) and quantitated by ImageMaster image analysis software (Amersham Biosciences).

Quantitative Reverse Transcriptase-PCR—RNase L$^{+/+}$ and *RNase L*$^{-/-}$ MEFs were treated with IFN-α (BDBB), 1000 units/ml for 4 h. Cells were then treated with 5 μg/ml actinomycin D for different periods of time. Cells were harvested, and total RNA was isolated with TRIzol reagent (Invitrogen). Five μg of total RNA was used to prepare cDNA with Superscript II reverse transcriptase (Invitrogen). Relative levels of PKR mRNA and glyceraldehyde-3-phosphate dehydrogenase mRNA were determined using quantitative PCR (Taqman assay) in an ABI Prism 7700 thermal cycler. PCR was performed for 40 cycles according to the manufacturer's protocol. Data analysis was done using Sequence detector version 1.7 software. Results were expressed as -fold difference compared with untreated samples. A rodent glyceraldehyde-3-phosphate dehydrogenase detection kit was obtained from PE Biosystems. PKR forward and reverse primers were prepared at Invitrogen. PKR probe dual-labeled with TAMRA and FAM was synthesized by Integrated DNA Technologies, Inc. (Coralville, IA). Primers and probes were selected using the Primer Express 1.0 software from ABI, Inc. The PKR forward primer sequence is 5′-GTT AAA GAG CCC GCC GAA A-3′, and the reverse primer sequence is 5′-CTG CTG GAA AAG CCA CTG AAT-3′, whereas the Taqman PKR probe is 5′-CTG CCG GAA CAT CCT CTA GCG TTG TC-3′.

Statistics, Image Analysis, and mRNA Decay Analysis—For comparison between two groups (columns on figures) the Student's paired *t* test was used. For comparisons among three groups of data (columns on figures), one-way analysis of variance (ANOVA) was used. Whereas, in evaluating two groups of data in consideration of other factors (*e.g.* in response to different doses of IFN), two-way ANOVA was used. Repeated-measures ANOVA was used for paired experiments. A paired Student's *t* test for comparison between two sets of paired data was performed. Two-tailed probabilities were reported. Densitometry, band detection, background subtraction, and normalization of images was performed using ImageMaster Software (Amersham Biosciences). The one-phase exponential decay curve analysis (GraphPad Prism) was used to assess mRNA decay kinetics. The equation, $y = \text{SPAN} \times e^{xK} \times \text{PLATEAU}$, describes the kinetics of mRNA decay. x is time, and y may be a concentration, binding, or response. y begins equal to SPAN + PLATEAU and decreases to PLATEAU with a rate constant K. The half-life of the decay is 0.6932/K. SPAN and PLATEAU are expressed in the same units as the y axis. K is expressed in the inverse of the units used by the x axis.

RESULTS

PKR Activity in the Presence and Absence of RNase L—During the course of experiments aimed at studying the role of RNase L in controlling protein synthesis during acute viral infections, regulation of PKR was monitored in *RNase L*$^{+/+}$ and *RNase L*$^{-/-}$ mouse embryonic fibroblast (MEF) cell lines by different methods. Initially, PKR assays were performed with poly(I)·poly(C) as activator and endogenous eIF2α as substrate in extracts of cells treated with IFN-α (1000 units/ml) for different periods of time. Phosphorylation of the α subunit of eIF2 was determined with a specific antibody. In wild type cells, PKR induction showed transient kinetics following IFN treatment, increasing 4-fold by 6 h and returning to baseline levels by 12 h (Fig. 1*A*). In contrast, in the *RNase L*$^{-/-}$ cells, PKR appeared with extended kinetics, remaining elevated at 36 h post-IFN addition. There were no changes in levels of total eIF2α in either cell type during IFN treatment (Fig. 1*A*, *middle panel*).

To confirm these findings, endogenous levels of eIF2α phosphorylation were determined in intact cells following EMCV infections. The levels of phosphorylated eIF2α were transiently increased in *RNase L*$^{+/+}$ cells following IFN treatment and infection with EMCV (Fig. 1*B*). In contrast, levels of phosphorylated eIF2α in infected *RNase L*-null cells peaked about 2-fold higher when compared with wild type cells (Fig. 1). In addition, after EMCV infections, phosphorylated eIF2α levels decreased rapidly in wild type cells while remaining elevated in *RNase L*$^{-/-}$ cells (Fig. 1, *A* and *B*).

To rule out indirect effects on eIF2α phosphorylation levels possibly mediated by phosphatases, we immunopurified PKR and measured its kinase activity using [γ-^{32}P]ATP. There was significantly increased PKR activity as determined by auto-

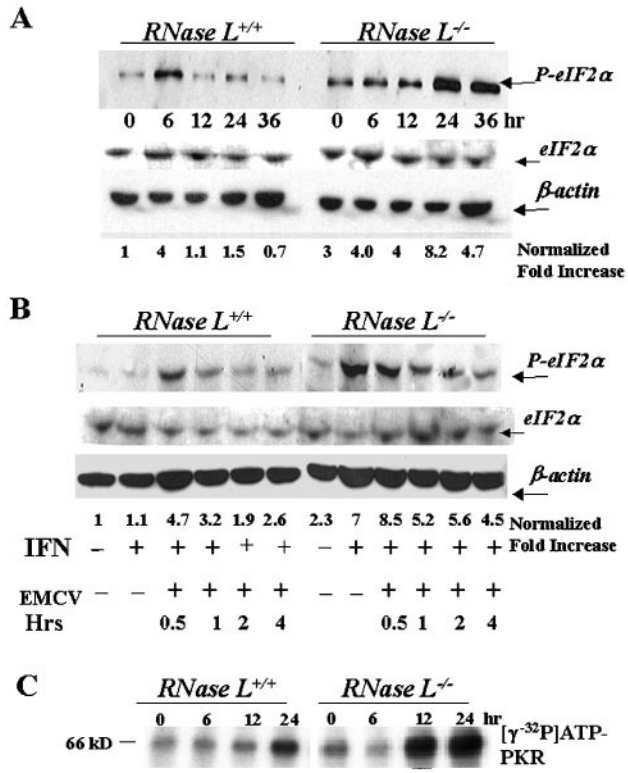

FIG. 1. **PKR-mediated eIF2α phosphorylation from *RNase L*$^{+/+}$ and *RNase L*$^{-/-}$ MEFs.** *A*, PKR activity was measured by monitoring the phosphorylation of eIF2α. Cells were treated with IFN-α (1000 units/ml) for the indicated periods of time except for control. Kinase assays were for 30 min at 30 °C in the presence of poly(I)·poly(C). Western blots were probed with antibodies specific to Ser-51-phosphorylated eIF2α and then detected by HRP-conjugated secondary antibody. *B*, cells were treated with and without IFN-α (1000 units/ml) for 16 h and subsequently infected with EMCV (m.o.i. of 10) for the indicated periods of time. Cell lysates were assayed for PKR activity on eIF2α without subjecting to kinase buffer (*e.g.* no ATP or poly(I)·poly(C)). Western blots for phosphorylated eIF2α were performed as described above. Bands were quantitated densitometrically, analyzed, and normalized to β-actin signals using ImageMaster Software. The -fold increase (compared with wild type cell control) was assessed using β-actin-normalized phosphorylated eIF2α levels while monitoring for total eIF2α. *C*, cells were treated with IFN-α (1000 units/ml) for the indicated periods of time except for control. Cell lysates were used to immunopurify PKR as explained under "Experimental Procedures." Kinase reactions with [γ-^{32}P]ATP and poly(I)·poly(C) were performed with the immunopurified PKR. Subsequently, the PKR were run on 12% PAGE and visualized by autoradiography.

phosphorylation in extracts of IFN-treated *RNase L*-null cells when compared with similarly treated wild type cells (Fig. 1*C*). Therefore, PKR activity as measured by these three approaches was found to be IFN induced to higher levels and for longer periods of time in the absence of RNase L.

Biological Consequences of RNase L Regulation of PKR on Viral Protein Synthesis—We chose encephalomyocarditis virus (EMCV) and vesicular stomatitis virus (VSV), RNA viruses that are sensitive to IFN-α, to determine the biological consequences of RNase L regulation of PKR (16, 17). Profiles of viral and cellular protein synthesis were determined by pulse labeling 1.5 h with [^{35}S]cysteine/methionine in the presence of actinomycin D to suppress host but not viral transcription (14, 15). IFN treatment inhibited viral protein while restoring synthesis of cellular proteins due to suppression of virus-induced shut-off of host cell protein synthesis (14, 15, 18, 19). At high multiplicities of infection (m.o.i. = 10 or 100), the viruses effectively shut-off cellular protein synthesis (Fig. 2, *A–C*; compare *lanes 2* to *1* and *lanes 5* to *4*). As a result of IFN treatment, there was partial anti-viral activity in wild type cells but not

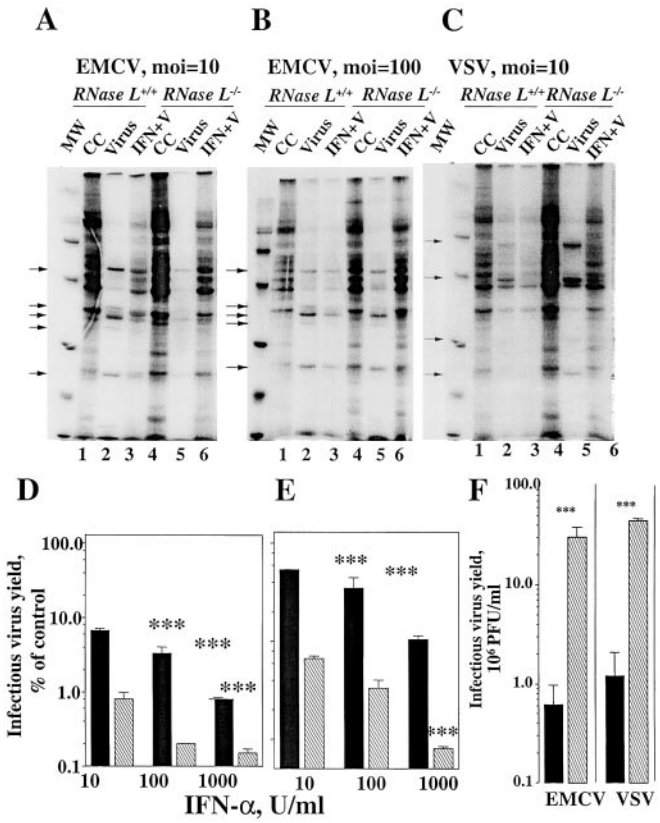

FIG. 2. **Inhibition of viral protein biosynthesis.** *RNase* $L^{+/+}$ MEFs and *RNase* $L^{-/-}$ MEFs were treated with mock (cell control; *CC*), virus (*V*), or IFN (1000 units/ml) for 20 h followed by virus (*IFN+V*). Viruses are EMCV at m.o.i. of 10 (*A*), EMCV at m.o.i. of 100 (*B*), and VSV at m.o.i. = 10 (*C*). Protein synthesis in the presence of actinomycin D, which inhibits cellular but not viral RNA synthesis, was monitored as described under "Experimental Procedures"; equal amounts of lysates were loaded onto SDS-PAGE. *MW*, molecular mass standards (220, 97.4, 66, 46, 30, 21.5, and 14.3 kDa). Representative autoradiograms from three experiments are shown. *Arrows* indicate positions of viral proteins. *RNase* $L^{+/+}$ MEFs (*black columns*) and *RNase* $L^{-/-}$ MEFs (*hatched columns*) were first treated with IFN-α (1000 units/ml, 20 h) except control and infected with EMCV (*D*) or VSV (*E*). Infectious virus yields were measured as described under "Experimental Procedures." Data are the average ± S.E. of three independent experiments and represented as percentage of control (untreated cells, 100%). *F*, virus yield in absence of IFN in *RNase* $L^{+/+}$ MEFs (*black columns*) and *RNase* $L^{-/-}$ MEFs (*hatched columns*) from three experiments. *Bars* denote S.E. ***, statistical significance at $p < 0.001$, using Student's paired *t* test when comparing *RNase* $L^{+/+}$ to *RNase* $L^{-/-}$ cell results.

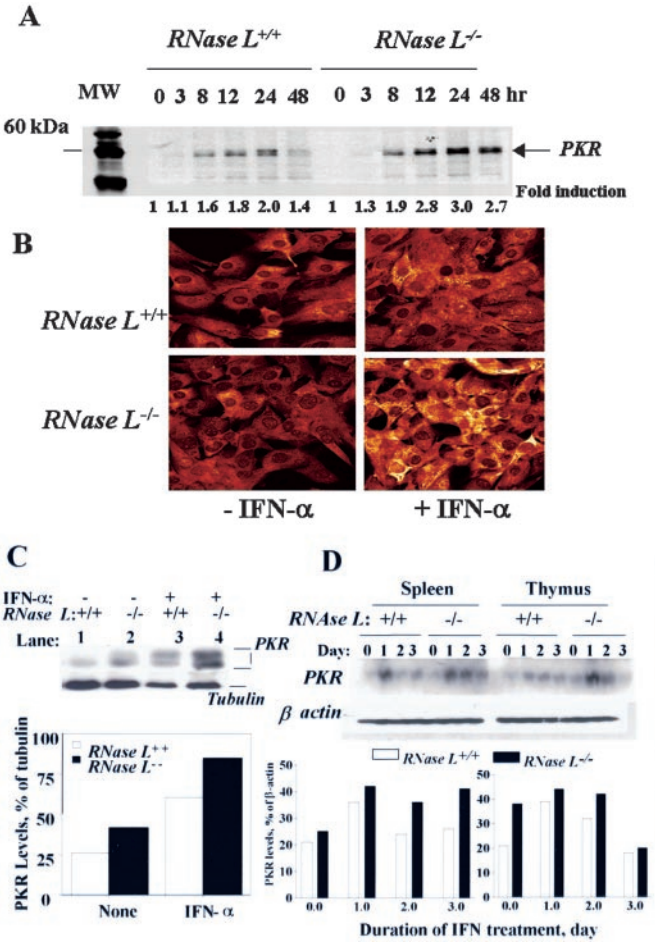

FIG. 3. **PKR levels in *RNase L*-null and wild type cells.** *A*, MEFs were treated with IFN-α (1000 units/ml) for the indicated periods of time, except for control (0 h), in media containing [^{35}S[methionine. PKR was immunoprecipitated from cell lysates and visualized in autoradiograms. *B*, confocal microscopy images of PKR induction. Semi-confluent MEF lines were treated with 1000 units/ml IFN-α for 18 h, followed by fixing and staining with primary antibodies to PKR. The fluorescein isothiocyanate-labeled secondary antibodies were used to reveal the primary antibody against PKR and thus indirectly visualize the PKR protein. *C*, PKR levels were determined in immunoblots from control or IFN-α-treated (2000 units/ml for 24 h) bone marrow macrophages of *RNase* $L^{+/+}$ (C57BL/6) and *RNase* $L^{-/-}$ mice of the same genetic background. The *lower panel* represents graphical representation of data from the *upper panel*. PKR levels are shown as a percentage of the relative levels of tubulin. *D*, organs (spleen and thymus) were excised from *RNase* $L^{+/+}$ and *RNase* $L^{-/-}$ mice after intraperitoneal injection of 10^5 units/ml IFN-α for the indicated periods of time. Western blots were performed using antibodies to PKR and β-actin.

enough to completely relieve virus-induced blockage of cellular protein synthesis (Fig. 2, *A–C*, *lane 3*). IFN-α alone had no significant effect on cellular protein synthesis in either cell type (data not shown). Remarkably, the inhibition of EMCV protein synthesis (m.o.i. of 10) was more potent in *RNase* $L^{-/-}$ than in *RNase* $L^{+/+}$ cells (Fig. 2, *A* and *B*), and the IFN was able to both inhibit viral protein synthesis and significantly restore cellular protein synthesis (Fig. 2, *A* and *B*, *lane 6*). The effect was even more apparent at the higher m.o.i. of 100 (Fig. 2*B*). Similar findings were observed with VSV, viral shut-off of host translation was prevented by IFN treatment of *RNase L*-null cells but not of wild type cells (Fig. 2*C*). The antiviral activity of IFN-α in wild type and *RNase* $L^{-/-}$ cells was determined in viral yield reduction plaque assays on indicator cells. Confluent cells were pretreated with different amounts of IFN-α (10–1000 units/ml) and subsequently infected at an m.o.i. of 10. At this high m.o.i., the anti-EMCV and VSV action of IFN-α was actually superior ($p < 0.005$, ANOVA) in *RNase* $L^{-/-}$ MEFs compared with wild type MEFs (Fig. 2, *D* and *E*). For example, at a dose of 1000 units/ml of IFN-α, there was 100-fold inhibition in infectious EMCV yield from *RNase L* $^{-/-}$ MEFs compared with only 8-fold inhibition in EMCV yield ($p < 0.0001$, Student's paired *t* test) from wild type cells (Fig. 2*D*). The enhanced action against viral protein biosynthesis was conditional on the IFN response, because in the absence of IFN, virus yield was higher from *RNase L*-null cells when compared with wild type cells (Fig. 2*F*). There was 40- to 50-fold greater virus yield ($p < 0.001$, Student's paired *t* test) in *RNase* $L^{-/-}$ MEFs when compared with wild type MEFs.

PKR Levels in Different Cell Types in Culture and in Mice—To determine whether the extended kinetics of phosphorylated eIF2α in IFN-treated RNase $L^{-/-}$ were due to PKR, levels of PKR protein were determined (Fig. 3*A*). IFN induction of PKR was increased with extended kinetics (up to 48 h) in the *RNase L*-null cells compared with IFN-treated wild type cells (Fig. 3*A*). The PKR protein levels peaked much later than PKR activity (Fig. 1*A*) suggesting an additional level of regulation

(20). The increased PKR protein levels due to absence of RNase L were further confirmed with confocal microscopy showing increased immunostaining of IFN-induced levels of PKR protein in *RNase* $L^{-/-}$ cells when compared with wild type cells (Fig. 3*B*).

To rule out cell type differences and concurrently confirm the PKR up-regulation *in vivo*, we performed experiments in primary cells and in mice organs. Primary macrophages isolated from bone marrow were cultured in the absence or presence of IFN-α for 24 h (Fig. 3*C*). Levels of PKR, normalized to tubulin levels, were modestly increased (1.4- to 1.6-fold) in the *RNase* $L^{-/-}$ macrophages compared with wild type macrophages, regardless of the presence of IFN (Fig. 3*C*). IFN induction of PKR was about 2-fold in *RNase* $L^{-/-}$ and wild type macrophages.

To determine PKR levels *in vivo*, mice were injected intraperitoneal with IFN-α (10^5 units/ml) for different times prior to sacrificing. Western blots of thymus and spleen proteins were then probed with antibody to PKR (Fig. 3*D*). In spleens of the *RNase* $L^{-/-}$ mice, PKR levels remained elevated (by 1.4-fold) until 48 h after IFN treatment, in contrast to the *RNase* $L^{+/+}$ mice in which PKR levels returned nearly to baseline at this time point (Fig. 3*D*). In thymus glands, PKR reached 1.7-fold higher levels by 16 h of IFN treatment in the *RNase* $L^{-/-}$ mice compared with IFN treated wild type mice (Fig. 3*D*). These experiments confirm extended PKR levels due to absence of RNase L in primary cells of different types.

Transient Transfections of RNase L cDNA Inhibit PKR Induction in Human Cells—To overexpress RNase L, we used the human cell line, WISH (HeLa markers), which achieved high transfection efficiency (~85%) as observed with green fluorescent protein vector (data not shown). In contrast, the *RNase L*-null mouse fibroblasts show low transfection efficiency. The transient expression of human RNase L cDNA in WISH cells caused abrogation of IFN-induced PKR protein as assessed with confocal microscopy using specific antibody to PKR (Fig. 4*A*). Western blots showed that overexpression of RNase L caused reductions of constitutive (40% β-actin-normalized reduction) and IFN-induced PKR protein (70% β-actin-normalized reduction) (Fig. 4, *B* and *C*). Generally, staining cells with fluorescence-labeled antibodies (confocal microscopy, Fig. 4*A*) gave lower background than Western blotting (Fig. 4B), because the latter involved denaturation in SDS-PAGE. The RNase L-induced effect on PKR protein levels correlated with PKR mRNA levels (Fig. 4, *D* and *E*), there was about 60% β-actin normalized reduction in IFN-induced PKR mRNA levels (Fig. 4, *D* and *E*).

RNase L Does Not Regulate PKR Expression and Kinetics by Influencing IFN Signaling—To elucidate the mechanism of PKR overexpression and/or prolongation in *RNase* $L^{-/-}$ cells, we determined PKR mRNA levels and stability of *RNase* $L^{-/-}$ and RNase $L^{+/+}$ cells as a function of time of IFN treatment. Indeed, in *RNase* $L^{-/-}$ MEFs there was enhanced and prolonged expression of PKR mRNA in *RNase* $L^{-/-}$ cells in contrast to the transient and much lower levels observed in wild type cells (Fig. 5, *A* and *B*). The data showed that PKR mRNA was induced to about 3-fold higher levels in the *RNase* $L^{-/-}$ cells and remained elevated after 24 h. In contrast, PKR mRNA levels returned to baseline amounts by 24 h in wild type cells (Fig. 5, *A* and *B*). Levels of β-actin mRNA and rRNA, monitored for comparison, were unaffected by the absence of RNase L (Fig. 5, *A* and *C*). To determine if enhanced IFN signaling was responsible for the overexpression of PKR mRNA, we monitored tyrosine phosphorylation of STAT-1 and receptor-mediated acidification rates (Fig. 5, *D* and *E*). In both cell types, there was STAT-1 phosphorylation due to IFN treatment, but no significant differences in the levels of phosphorylated

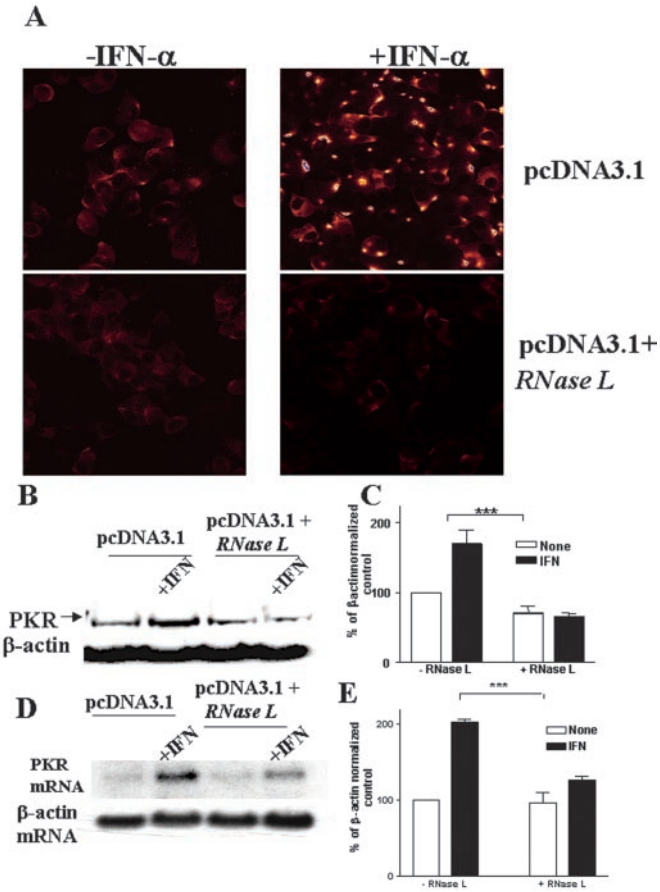

FIG. 4. **Exogenous expression of RNase L in human cells.** Semiconfluent (75%) WISH (HeLa markers) cells, which assume high transfection efficiency (~85% as assessed by green fluorescent protein vector), were transfected using LipofectAMINE 2000 as described under "Experimental Procedures" with either pcDNA3.1 vector as a control or pcDNA3.1 expressing the full-length human RNase L cDNA. After about 24 h, cells were treated with human IFN-α2a (500 IU/ml) for 18 h. *A*, cells were stained with anti-PKR followed by fluorescently labeled antibody for visualization under confocal microscopy. *B*, cells were used for Western blotting using antibodies to PKR and β-actin. The -fold differences between untreated vector-transfected and other lanes were quantitated densitometrically and normalized to β-actin signals using ImageMaster Software (*C*). Cells were also used for Northern blotting using cDNA to human PKR and also β-actin (*D*). Lanes from two independent experiments were quantitated densitometrically and normalized to β-actin signals using ImageMaster Software (*E*). Mean ± S.D. were shown in both graphs. ***, $p < 0.001$ as assessed by ANOVA.

STAT-1 exist between wild type and *RNase* $L^{-/-}$ cells (Fig. 5*D*). Additionally, we used the Cytosensor microphysiometer system (CMS), which is a biosensor capable of measuring minute changes in extracellular acidification due to the receptor activation in living cells (21). Both types of cells were placed in the CMS in low buffered running medium, and the acidification rates were monitored until stable baseline rates were obtained. After equilibrium, cells were exposed to IFN-α for 2 min. The acidification rates due to IFN-α treatment were monitored until returning to baseline (Fig. 5*E*). We were able to measure activation of the cells owing to IFN-α addition in real-time and found that peak acidification occurred in only 3.3 min. The responses to either type of cells are transient, *i.e.* rapidly return to the baseline (Fig. 5*E*). We noted that there were no detectable differences in the peaks, acidification rates, or decay of the IFN response between the wild type and *RNase* $L^{-/-}$ MEFs.

PKR mRNA Stability Is Affected by the Presence or Absence of RNase L—To determine if the effect of RNase L on PKR mRNA levels was at the level of mRNA turnover, we blocked transcrip-

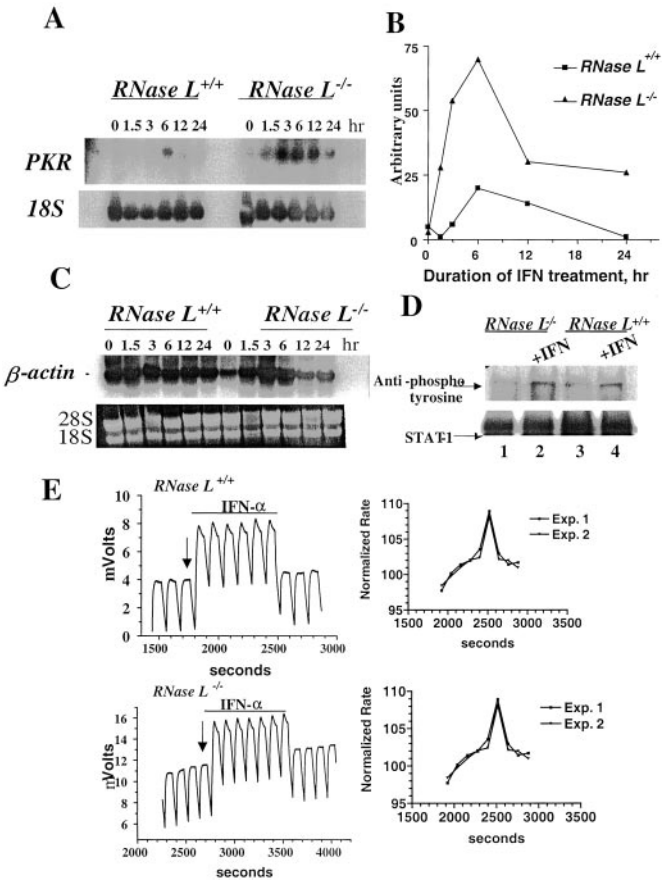

FIG. 5. **Effects of RNase L on kinetics and signaling of PKR mRNA induction.** *RNase L*$^{+/+}$ and *RNase L*$^{-/-}$ MEFs were treated with IFN-α (1000 units/ml) for the indicated periods of time. *A*, RNA was probed for PKR mRNA (*upper panel*) or 18 S RNA (*lower panel*). *B*, the kinetics of PKR induction are shown graphically as arbitrary densitometric units (minus background). *C*, Northern blotting using β-actin as a probe (*upper panel*); loading was verified by ethidium bromide of 18/28 S RNA (*lower panel*). *D*, *RNase L*$^{-/-}$ (*lanes 1* and *2*) and *RNase L*$^{+/+}$ (*lanes 3* and *4*) MEFs were treated briefly (15 min) with IFN-α (1000 units/ml; *lanes 2* and *4*). Cells were lysed and immunoprecipitated with anti-STAT-1 followed by Western blotting using anti-phosphotyrosine antibody. Equal amounts of lysates were loaded into each lane as verified by total STAT-1 proteins visualized in the immunoblot of the gel (*lower panel*). *E*, functional response to IFN-α using Cytosensor microphysiometer system (CMS) were determined in *RNase L*$^{+/+}$ and *RNase L*$^{-/-}$ MEFs. The graphs show raw data, millivolt changes over time, whereas smaller graphs (*insets*) show the acidification rate (percentage of the baseline) normalized to the baseline (100%). The *vertical arrows* indicate the addition of IFN-α.

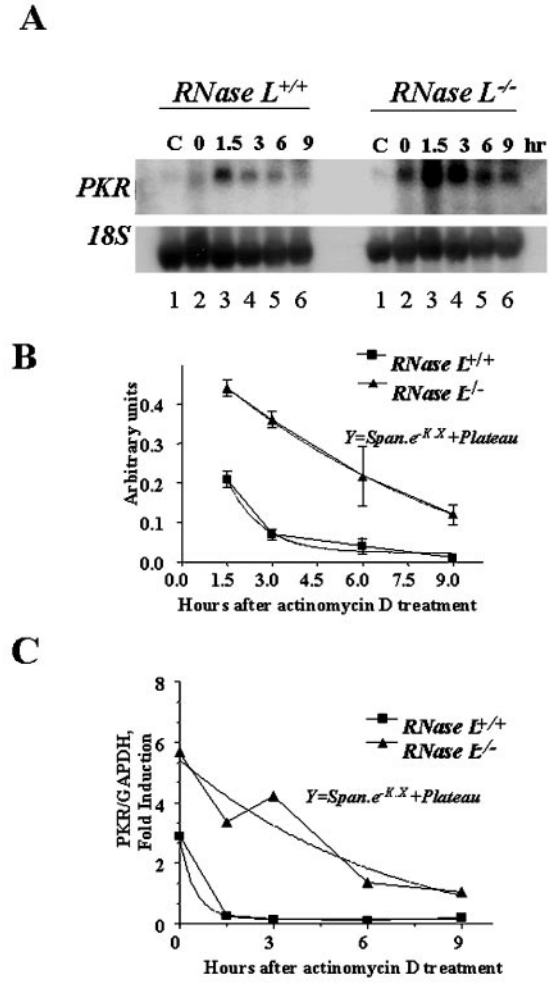

FIG. 6. **Influence of RNase L on PKR mRNA stability.** *A*, *RNase L*$^{+/+}$ and *RNase L*$^{-/-}$ MEFs were treated with medium control (*lane 1*) or IFN-α (1000 units/ml, *lane 2*) for 4 h followed by actinomycin D (5 μg/ml) for various times (*lanes 3–6*) as indicated. The *upper* and *lower panels* are Northern blots for PKR mRNA and 18 S rRNA, respectively. *B*, one-phase exponential decay curves from three independent experiments with S.E. *bars* are shown; densitometric units (minus background) are plotted as a function of time after addition of actinomycin D. *C*, *RNase L*$^{+/+}$ and *RNase L*$^{-/-}$ MEFs on C57BL/6 genetic background were treated with IFN-α (1000 units/ml) for 4 h and subsequently treated with 5 μg/ml actinomycin for various intervals. Total RNA was extracted, reverse-transcribed, and subjected to quantitative PCR (Taqman assay) for determination of relative levels of PKR mRNA and glyceraldehyde-3-phosphate dehydrogenase mRNA. One-phase exponential decay analysis was applied on decaying signals to determine relative mRNA half-life changes in the two cell types are shown. x is time, and y is mRNA levels in arbitrary densitometric units. y starts out equal to SPAN plus PLATEAU and decreases to PLATEAU with a rate constant K. The half-life of the decay is $0.6932/K \times$ SPAN and PLATEAU are expressed in the same units as the y axis. K is expressed in the inverse of the units used by the x axis.

tion with actinomycin D. There was an initial increase in PKR mRNA levels in both types of cells when assessed at 1.5 h probably due to the effect of inhibiting synthesis of labile transacting proteins (Fig. 6). Similar effects are observed for some AU-rich mRNAs (22, 23). The initial increase in PKR mRNA amounts was consistently observed ($n = 4$) and thus was not due to cell culture or experimental variations. We performed one-phase exponential decay kinetics analysis 1.5 h after addition of actinomycin D. PKR mRNA decay rates and relative differences between *RNase L*$^{+/+}$ and *RNase L*$^{-/-}$ cells were thus determined. The analysis revealed that the half-lives of PKR mRNA in *RNase L*$^{-/-}$ MEFs was 6.7 h compared with only 0.8 h in *RNase L*$^{+/+}$ cells (Fig. 6, *A* and *B*). Thus, PKR mRNA had an 8-fold increased half-life in the *RNase L*$^{-/-}$ cells (Fig. 6*B*). The constant rate (K) measurements indicated that the PKR mRNA decay rate is slower in *RNase L*$^{-/-}$ ($K = 0.1$) than wild type cells ($K = 0.8$). Furthermore, we used independently derived cell lines from *RNase L*$^{+/+}$ and *RNase L*$^{-/-}$ mice, both on a genetic background of C57BL/6, to rule out possible nonspecific cell line differences to assess PKR mRNA stability. A real-time PCR assay was used to measure the half-life of the PKR mRNA (Fig. 6*C*). Relative results were similar to that obtained by Northern blot assays. Specifically, the half-life of PKR mRNA was 4.6 h in *RNase L*$^{-/-}$ cells compared with 0.4 h in wild-type cells.

DISCUSSION

Our findings demonstrate that the 2-5A/RNase L system negatively regulates PKR expression. A deficiency in RNase L produces enhanced and prolonged IFN induction of PKR due to increased half-life of PKR mRNA. The PKR mRNA stabiliza-

TABLE I
Antiviral IFN action in cell and animals deficient in RNase L, PKR, or both

Data are compiled from prior studies (12, 25) (Footnotes *a–c*) and this study (Footnote *d*). Down arrows denote reduction of antiviral action of IFN whereas up arrows denote increased IFN action in gene- knock-out models in comparison to wild type controls. Two arrows indicate stronger effects than one arrow whereas **0** denotes either no effect or statistically not significant.

Genotype	Cells Low MOI [a,c]	Cells High MOI [b,d]	Animals [a]
$PKR^{-/-}$ vs $PKR^{+/+}$	↓	↓	0↓
$RNase\ L^{-/-}$ vs. $RNase\ L^{+/+}$	0↓	↑↑ [d]	0↓
$PKR^{-/-}RNase\ L^{-/-}$ vs. $PKR^{+/+}RNase\ L^{+/+}$	↓↓	↓↓	↓↓

tion appears to be selective and not due to global mRNA stabilization. Furthermore, in IFN-α-treated EMCV-infected *RNase* $L^{-/-}$ cells, elevated levels of PKR correlate with enhanced eIF2α phosphorylation and superior inhibition of virus replication. We consistently observed enhanced and/or prolonged IFN induction of PKR in the absence of RNase L regardless of the cell type, genetic background, and whether experiments were performed in cell culture or in animals. Also, transient expression of human RNase L in human cells caused selective abrogation of both constitutive and IFN-induced PKR expression. Taken together our results suggest that RNase L negatively modulates the IFN antiviral response and that the transient appearance of phosphorylated eIF2α under some conditions (*e.g.* viral infections at high m.o.i. values) is, at least partly, a result of the negative feedback mechanism imparted by RNase L.

RNase L Regulation and Inhibition of Viral Protein Synthesis—PKR action mediates translational arrest in host cells through phosphorylation of eIF-2α and has been previously implicated in innate immunity to EMCV (24, 25), VSV (26), and HSV-1 (17). Mice deficient in PKR have somewhat reduced antiviral responses to IFNs (26, 27), and notably PKR-deficient cells are prone to HSV-1 infection (17). Thus, PKR-mediated eIF-2α phosphorylation acts as mechanism in antiviral immunity during the IFN response but has also been implicated in a variety of responses induced by growth factor deprivation, oxidative stress, the proinflammatory cytokine tumor necrosis factor-α, bacterial lipopolysaccharides, and viral (dsRNA) products (28–30). The biological consequence of the extended kinetics of PKR mRNA expression in the absence of RNase L is reflected in levels of phosphorylated eIF2α. Subsequently, this led to the enhanced inhibition of viral protein synthesis confirming the importance of the PKR/eIF-2α pathway in controlling viruses. Nevertheless, alternative antiviral IFN-stimulated pathways other than PKR might also be affected by the absence of RNase L.

IFN induction of PKR was significantly increased in *RNase L*-null cell lines and modestly increased in primary macrophages and organs isolated from the *RNase L*-null animals compared with similarly treated wild type cells and mice. Modest increases of PKR in animals as opposed to cells in culture may be due to the *in vivo* occurrence of low levels of IFN that would reduce the magnitude of induction. It has been suggested that PKR may participate in the autocrine production of IFN (24, 26). This may explain the occasional presence of higher PKR levels in non-IFN-stimulated cells such as those of primary macrophages isolated from *RNase L*-null mice. It is unlikely, however, that increased autocrine production of IFN is responsible for the extended translational arrest in IFN-treated *RNase L*-null cell line, because the viral protein synthesis assay was performed within 4 h of virus infection in the presence of the transcriptional blocker, actinomycin D. The exogenous expression of human RNase L in human epithelial cell line (WISH, HeLa markers) not only extends the findings of murine cells to human cells, murine and human and murine RNase L share 64% amino acid homology (31), but also offers a direct link between RNase L and PKR pathways.

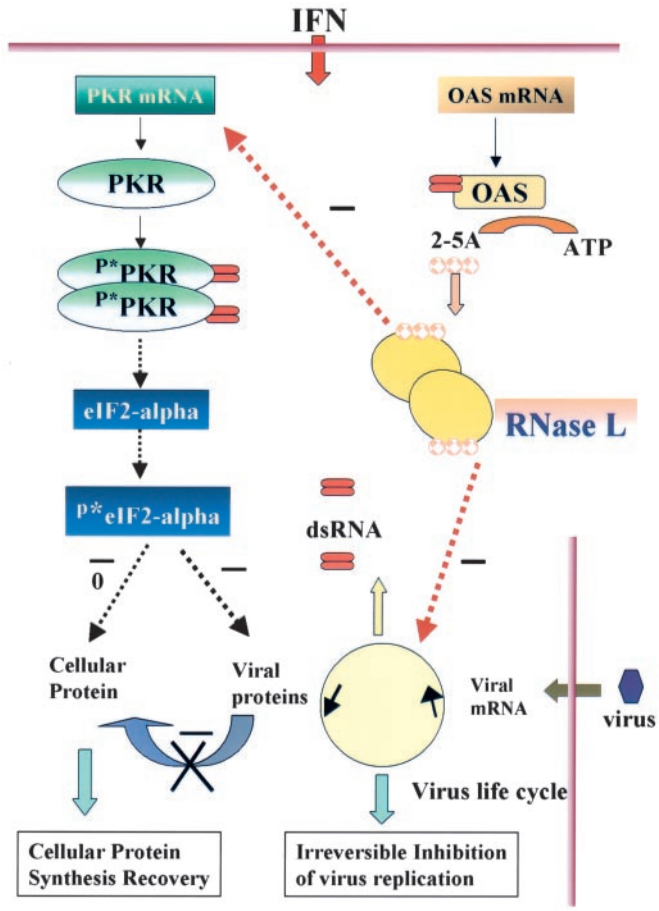

FIG. 7. **A scheme depicting the IFN antiviral response.** Upon infection, viruses shut-off cellular, usually cap-dependent protein synthesis (Fig. 2, *A–C*; *lanes 2* and *5*) by several mechanisms, including disturbance of eIF4G and eIF4E (18, 19, 44, 45) so that cap-independent viral protein synthesis can proceed (*blue block arrow*, *bottom*). As a first line of defense, the host intracellular enzymes themselves, RNase L and PKR, act by degrading viral mRNA and inhibiting viral protein syntheses, respectively, as demonstrated by gene knockout studies (12, 17, 25, 27) (Fig. 2*F*). IFN, which has been produced during the early phase of infection before cells are compromised by the virus, now comes into play to protect surrounding cells from viral attack. IFN induces further PKR and 2′,5′-oligoadenylate synthetase (*OAS*). The viral double-stranded RNA (*dsRNA*) acts as an activator for both PKR and OAS/RNase L pathways. dsRNAs binds and activates PKR, which phosphorylates itself, and subsequently phosphorylates eIF2α. The phosphorylated eIF2α leads to inhibition of viral protein synthesis (Fig. 2, *A–D*) but may also cause transient and modest inhibition of cellular protein synthesis. However, the latter is rapidly restored because inhibition of viral protein synthesis (*a*) serves to relieve the virus-induced blockage of protein synthesis from capped mRNA and as a result rapid replacement of mRNAs (and proteins) (*b*) from the host's genome (Fig. 2, *A–C*; *lanes 3* and *6*). When activated by dsRNA, OAS converts ATP to 2′,5′-oligoadenylate (*2-5A*). This product activates RNase L, which selectively degrades viral mRNA (10). In the presence of IFN, RNase L degrades PKR mRNA as demonstrated by RNase L-knockout studies (Figs. 5 and 6) and subsequently down-modulates PKR protein (Figs. 3 and 4) and eIF2α phosphorylation (Fig. 1) to prevent adverse prolonged response so that healthy cells survive after virus clearance. The *dash* denotes inhibitory action.

RNase L Regulation of PKR Pathway—Our data show that the RNase L-mediated regulation of PKR pathway is operative

during IFN response (Fig. 2). This may not be the case, however, with overexpression of RNase L, which resulted in significant reduction of both constitutive and IFN-induced PKR. This may be due to the fact that transfected cells release small amounts of IFN. Another requirement for the enhanced inhibition of viral protein synthesis is high multiplicity of infection (m.o.i.). This is concluded from the reconciliation of previous findings (12, 25) with the findings of this paper. Previously, low m.o.i. conditions (*e.g.* m.o.i. = 0.01) resulted in viral yields that were either nearly identical or modestly reduced in IFN-treated *RNase L*-null cells compared with wild type cells. In this report, we used high m.o.i. (10 or 100). The RNA-PKR interaction is complex and is dependent on concentration, length, and structure of dsRNA molecules. PKR levels and optimum interactions are necessary for dimerization of PKR for full activity (32–36). Thus, at high m.o.i., the combination of elevated levels of both viral dsRNA intermediates and IFN-induced PKR accounts for enhanced translational arrest leading to superior antiviral action of IFN-α in *RNase L*-null cells. Indeed, m.o.i. of 100 resulted even in stronger translational arrest than m.o.i. of 10 (Fig. 2, *A* and *B*). In acute infections, high m.o.i., such as those used in this study, may be more representative of an ongoing acute infection than experiments with low m.o.i. Very high levels of dsRNA (*e.g.* >10 μg/ml) inhibit PKR (35), but these levels do not appear to be obtained *in vivo*. Conversely, at low m.o.i., antiviral effects of elevated PKR may not be observed due to insufficient dsRNA. Table I summarizes *in vivo* and cell culture studies on *RNase L* and *PKR* gene disruption experiments, whereas Fig. 7 shows an overall scheme of the translational arrest during IFN response to acute virus infection, including the negative regulation of PKR pathway by RNase L reported here.

Regulation of Cellular mRNA by RNase L—The enhanced expression of PKR in the absence of RNase L was related to increased stability of PKR mRNA (Fig. 6). It is unlikely that these effects are due to changes upstream from mRNA expressions such as signaling, because there were no notable changes in the functional response of the cells to IFN-α as measured by the microphysiometer system Cytosensor or STAT-1 phosphorylation, the latter event being necessary to the STAT-JAK pathway-mediated transcription of IFN-stimulated genes (37). For RNase L to degrade mRNAs, it needs to be activated by 2-5A (Fig. 7). These results suggest that 2-5A is present in cells treated with IFN but in the absence of viral infections. It is possible that low levels of dsRNA capable of weakly activating 2-5A synthetase are present among cellular RNA (38, 39) leading to generation of low levels of 2-5A. It was previously suggested that RNase L, itself, does not cause global degradation of cellular mRNA in intact cells due to low levels of 2-5A, and only 2-5A at rather high concentrations, is needed to degrade cellular mRNA such as ribosomal RNA (10, 11, 40). Indeed, our data show that changes in the PKR mRNA expression are specific when compared with β-actin mRNA and ribosomal RNA expression. Also, differential display analysis showed that there were no general cellular mRNA profile changes as a result of RNase L deficiency.[2] Two recent studies showed that the mRNA stability of ubiquitin-specific protease mRNAs termed ISG43 and ISG15 mRNA were enhanced in *RNase L*-null cells, but this has not been correlated with IFN action (41). In a separate study (42), it has been concluded that an effect of RNase L on myoblast determination protein 1 mRNA levels was relatively specific, because expression of several other mRNAs was not altered in RNase L inhibitor-transfected HP68 cells. Also, it has been shown that RNase L degrades mitochondrial mRNAs for cytochrome *b*, ATPase 6, and cytochrome oxidase subunit II, but not glyceraldehyde-3-phosphate dehydrogenase mRNA (which was used as a control) (43). Taken together, the three studies, including ours, provide evidence for a restricted repertoire of RNase L cellular mRNA targets as opposed to global cellular mRNA regulation by RNase L. However, it remains to be determined whether RNase L selectively affects the turnover of specific sets of mRNAs in the cell.

Our findings support a novel role for RNase L in the control of PKR mRNA stability and therefore, in the transient regulation of PKR levels in IFN-treated cells. The control of mRNA stability is one mechanism that ensures the transient nature of processes such as immune response, cellular growth, differentiation, and responses to external stimuli. RNase L-induced transient responses of PKR activation may be a means of avoiding induction of stress pathways (*e.g.* activation transcription factor) elicited by eIF2α phosphorylation. Results suggest that RNase L may mediate the negative regulation of the IFN response during acute viral infections and perhaps in other cellular stress responses.

Acknowledgments—We thank Maud Dzimiri, Fehmina Chaudhry, and Saod Saleh for excellent technical assistance. We also thank Dr. Katherine Collison for reviewing the manuscript.

[2] K. S. A. Khabar, Y. M. Siddiqui, F. al-Zoghaibi, L. al-Haj, M. Dhalla, A. Zhou, B. Dong, M. Whitmore, J. Paranjape, M. N. Al-Ahdal, F. Al-Mohanna, B. R. G. Williams, and R. H. Silverman, unpublished results.

REFERENCES

1. Greenhalgh, C. J., and Hilton, D. J. (2001) *J. Leukoc. Biol.* **70,** 348–356
2. Bakheet, T., Frevel, M., Williams, B. R. G., Greer, W., and Khabar, K. S. A. (2001) *Nucleic Acids Res.* **29,** 246–254
3. Meurs, E., Chong, K., Galabru, J., Thomas, N. S., Kerr, I. M., Williams, B. R., and Hovanessian, A. G. (1990) *Cell* **62,** 379–390
4. Panniers, R., and Henshaw, E. C. (1983) *J. Biol. Chem.* **258,** 7928–7934
5. Meurs, E. F., Watanabe, Y., Kadereit, S., Barber, G. N., Katze, M. G., Chong, K., Williams, B. R., and Hovanessian, A. G. (1992) *J. Virol.* **66,** 5804–5814
6. Kerr, I. M., and Brown, R. E. (1978) *Proc. Natl. Acad. Sci. U. S. A.* **75,** 256–260
7. Silverman, R. H. (1997) in *Ribonucleases: Structure and Function* (D'Alessio, G., and Riordan, J. F., eds) pp. 515–551, Academic Press, New York
8. Biron, C. A., and Sen, G. C. (2001) in *Fields Virology* (Knipe, D. M., and Howley, P. M., eds) 4th Ed., pp. 321–352, Lippincott Williams & Wilkins Publishers, Philadelphia
9. Stark, G. R., Kerr, I. M., Williams, B. R., Silverman, R. H., and Shreiber, R. D. (1998) *Annu. Rev. Biochem.* **67,** 227–264
10. Li, X. L., Blackford, J. A., and Hassel, B. A. (1998) *J. Virol.* **72,** 2752–2759
11. Wreschner, D. H., James, T. C., Silverman, R. H., and Kerr, I. M. (1981) *Nucleic Acids Res.* **9,** 1571–1581
12. Zhou, A., Paranjape, J., Brown, T. L., Nie, H., Naik, S., Dong, B., Chang, A., Trapp, B., Fairchild, R., Colmenares, C., and Silverman, R. H. (1997) *EMBO J.* **16,** 6355–6363
13. Gangemi, J. D., Lazdins, J., Dietrich, F. M., Matter, A., Poncioni, B., and Hochkeppel, H. K. (1989) *J. Interferon. Res.* **9,** 227–237
14. Lewis, J. A. (1987) in *Lymphokines and Interferons: A Practical Approach* (Clemens, M. J., Morris, A. J., and Gearing, A. J. H., eds) pp. 73–87, IRL Press, Oxford
15. Mestan, J., Digel, W., Mittnacht, S., Hillen, H., Blohm, D., Moller, A., Jacobsen, H., and Kirchner, H. (1986) *Nature* **323,** 816–819
16. Khabar, K. S., Al-Zoghaibi, F., Al-Ahdal, M. N., Murayama, T., Dhalla, M., Mukaida, N., Taha, M., Al-Sedairy, S. T., Siddiqui, Y., Kessie, G., and Matsushima, K. (1997) *J. Exp. Med.* **186,** 1077–1085
17. Khabar, K. S., Dhalla, M., Siddiqui, Y., Zhou, A., Al-Ahdal, M. N., Der, S. D., Silverman, R. H., and Williams, B. R. (2000) *J. Interferon Cytokine Res.* **20,** 653–659
18. Gan, W., and Rhoads, R. E. (1996) *J. Biol. Chem.* **271,** 623–626
19. Gingras, A. C., Svitkin, Y., Belsham, G. J., Pause, A., and Sonenberg, N. (1996) *Proc. Natl. Acad. Sci. U. S. A.* **93,** 5578–5583
20. Hovanessian, A. G., Galabru, J., Meurs, E., Buffet-Janvresse, C., Svab, J., and Robert, N. (1987) *Virology* **159,** 126–136
21. Pitchford, S., Hirst, M., Wada, H. G., Chan, S. D., Timmermans, V. E., and Humphries, G. M. (1997) *Methods Enzymol.* **288,** 84–108
22. Rajagopalan, L. E., and Malter, J. S. (1996) *J. Biol. Chem.* **271,** 19871–19876
23. Chen, C. Y., Xu, N., and Shyu, A. B. (1995) *Mol. Cell. Biol.* **15,** 5777–5788
24. Yang, Y. L., Reis, L. F., Pavlovic, J., Aguzzi, A., Schafer, R., Kumar, A., Williams, B. R., Aguet, M., and Weissmann, C. (1995) *EMBO J.* **14,** 6095–6106
25. Zhou, A., Paranjape, J. M., Der, S. D., Williams, B. R., and Silverman, R. H. (1999) *Virology* **258,** 435–440
26. Balachandran, S., Roberts, P. C., Brown, L. E., Truong, H., Pattnaik, A. K., Archer, D. R., and Barber, G. N. (2000) *Immunity* **13,** 129–141
27. Der, S. D., and Lau, A. S. (1995) *Proc. Natl. Acad. Sci. U. S. A.* **92,** 8841–8845
28. Silverman, R. H., and Williams, B. R. (1999) *Nature* **397,** 208–209, 211
29. Patel, C. V., Handy, I., Goldsmith, T., and Patel, R. C. (2000) *J. Biol. Chem.*

275, 37993–37998
30. Der, S. D., Yang, Y. L., Weissmann, C., and Williams, B. R. (1997) *Proc. Natl. Acad. Sci. U. S. A.* **94,** 3279–3283
31. Zhou, A., Nie, H., and Silverman, R. H. (2000) *Mamm. Genome* **11,** 989–992
32. Wu, S., and Kaufman, R. J. (1997) *J. Biol. Chem.* **272,** 1291–1296
33. Pe'ery, T., and Mathews, M. B. (1997) *Methods* **11,** 371–381
34. Ehrenfeld, E., and Hunt, T. (1971) *Proc. Natl. Acad. Sci. U. S. A.* **68,** 1075–1078
35. Sharp, T. V., Xiao, Q., Jeffrey, I., Gewert, D. R., and Clemens, M. J. (1993) *Eur. J. Biochem.* **214,** 945–948
36. Patel, R. C., Stanton, P., McMillan, N. M., Williams, B. R., and Sen, G. C. (1995) *Proc. Natl. Acad. Sci. U. S. A.* **92,** 8283–8287
37. Darnel, J. J., Kerr, I., and Stark, G. (1994) *Science* **264,** 1415–1421
38. Hartmann, R., Norby, P. L., Martensen, P. M., Jorgensen, P., James, M. C., Jacobsen, C., Moestrup, S. K., Clemens, M. J., and Justesen, J. (1998) *J. Biol. Chem.* **273,** 3236–3246
39. Pratt, G., Galpine, A., Sharp, N., Palmer, S., and Clemens, M. J. (1988). *Nucleic Acids Res.* **16,** 3497–3510
40. Cirino, N. M., Li, G., Xiao, W., Torrence, P. F., and Silverman, R. H. (1997) *Proc. Natl. Acad. Sci. U. S. A.* **94,** 1937–1942
41. Li, X. L., Blackford, J. A., Judge, C. S., Liu, M., Xiao, W., Kalvakolanu, D. V., and Hassel, B. A. (2000) *J. Biol. Chem.* **275,** 8880–8888
42. Bisbal, C., Silhol, M., Laubenthal, H., Kaluza, T., Carnac, G., Milligan, L., Le Roy, F., and Salehzada, T. (2000) *Mol. Cell. Biol.* **20,** 4959–4969
43. Le Roy, F., Bisbal, C., Silhol, M., Martinand, C., Lebleu, B., and Salehzada, T. (2001) *J. Biol. Chem.* **276,** 48473–48482
44. Haghighat, A., Svitkin, Y., Novoa, I., Kuechler, E., Skern, T., and Sonenberg, N. (1996) *J. Virol.* **70,** 8444–8450
45. Kleijn, M., Vrins, C. L., Voorma, H. O., and Thomas, A. A. (1996) *Virology* **217,** 486–494

RNase L Mediates Transient Control of the Interferon Response through Modulation of the Double-stranded RNA-dependent Protein Kinase PKR

Khalid S. A. Khabar, Yunus M. Siddiqui, Fahad Al-Zoghaibi, Latifa Al-Haj, Mohammed Dhalla, Aimin Zhou, Beihua Dong, Mark Whitmore, Jayashree Paranjape, Mohammed N. Al-Ahdal, Futwan Al-Mohanna, Bryan R. G. Williams and Robert H. Silverman

J. Biol. Chem. 2003, 278:20124-20132.
doi: 10.1074/jbc.M208766200 originally published online February 11, 2003
